Braz J Phys (2016) 46:20–25
DOI 10.1007/s13538-015-0374-3

SOCIEDADE BRASILEIRA DE FÍSICA

CONDENSED MATTER

Realization of Graphene Physics Through a Fully Optical System

C. A. Dartora[1] · K. Z. Nobrega[2]

Received: 27 July 2015 / Published online: 9 November 2015

Abstract The two-dimensional form of carbon known as graphene awaken the scientific community interest due to its exotic electronic properties, emerging from the behavior of electrons near the Fermi level as massless Dirac fermions in a $(1 + 2)$-dimensional "relativistic" space-time, which renders a bridge between condensed matter and relativistic quantum field theory. Optical systems are also prodigal in providing analogues of complex quantum mechanical systems. Here, it is proposed an optical realization capable of capturing the essential physics of the Dirac equation in $(1+2)$-D dimensions, simulating the properties of graphene through the use of lightwave technology.

Keywords Graphene · Dirac equation · Optics · Mode coupling

1 Introduction

Enormous attention have been devoted to the study of the two-dimensional carbon allotrope known as graphene [1–6], due to its very unusual physical properties accompanied by the promise of revolutionizing the industry of high-speed nanoelectronics. The carbon atoms in graphene arrange in the form of a honeycomb lattice, leading to a very peculiar band structure which gives rise to an effective field theory of electrons emulating massless Dirac fermions in a $(1 + 2)$-dimensional Minkowski space-time, near the so-called Dirac points of the Brillouin zone [7–11]. The elusive relativistic character of electrons in graphene has been demonstrated by means of several experiments, such as the anomalous integer quantum Hall effect showing up even at room temperature at high magnetic fields [12, 13], and the Klein tunneling through a potential barrier, in which the higher the barrier height the more transparent it becomes for incident relativistic particles [14–19].

Meanwhile, the field of optics is prodigal in providing analogues of complex quantum mechanical systems. The efforts to construct optical analogues of quantum mechanics (QM) have been motivated by the fact that simpler optical systems can be used as analog computers, allowing to simulate the behavior of quantum mechanics in a more or less classical way. For instance, the best known examples of such analogies are the photonic crystals [20–24], which emulate the crystalline lattice of a solid. Additionally, the paraxial wave equation, emerging from the study of electromagnetic fields at optical frequencies in the so-called paraxial approximation, is the analogue of the non-relativistic Schrödinger equation of QM, with the role of time coordinate t in QM played by the longitudinal coordinate z in the paraxial equation [25, 26], and the study of Maxwell's equations in a weakly inhomogeneous medium provided an analogy between relativistic QM and optics [27]. Optical realizations of graphene and other artificial graphene-like structures have been proposed in the current literature [28–33]. A tight-binding model leading to artificial graphene was studied in ref. [29] using classical waves in the microwave domain, through the use of weakly coupled dielectric resonators arranged in honeycomb lattice, but the experiment is limited by losses and

✉ C. A. Dartora
cadartora@yahoo.com.br

[1] Electrical Engineering Department, Federal University of Parana (UFPR), Curitiba, Brazil

[2] Electrical Engineering Department, Federal Institute of Technological Education of Maranhão (IFMA), São Luis, Brazil

cavity quality factors. It was previously demonstrated that evanescent propagation of microwaves in dielectric resonators arranged in a honeycomb lattice is well described by a tight-binding model very similar to that describing electrons in graphene. The microwave setup also allows one to fine tuning the hopping parameters by changing the distance between the resonators [30]. In another approach to artificial graphene, metallic nanoparticles can be organized in a two-dimensional honeycomb lattices, supporting localized surface plasmons. The collective properties of plasmons are well described by a tunable plasmonic analogue of graphene [32]. Optical analogues of ballistic charge carriers in graphene were pointed out in ref. [33].

Our main goal in the present contribution is to demonstrate the possibility of an optical realization capable of capturing the essential physics of the Dirac equation in $(1+2)$-D dimensions, allowing one to simulate the properties of graphene through the use of lightwave technology.

The content of this article can be described as follows: in the next section, the emergence of the Dirac equation in $(1+2)$-D space-time will be carefully demonstrated in a simple optical system, through the use of coupled mode theory. To finish, in the last section, a few conclusions and remarks are added.

2 Emergence of Dirac's Equation in an Optical System

The electrons near the Fermi level in graphene are effectively described by the Dirac equation in a $(1+2)$-dimensional space-time [10, 11, 34, 35]:

$$i\hbar\gamma^\mu\partial_\mu\psi + e\gamma^\mu A_\mu\psi = 0, \tag{1}$$

where ψ is a two-component Dirac spinor, $A_\mu = (A_0, -A_x, -A_y)$ are the electromagnetic potentials in $1+2$-D space-time, and $e = 1.6\times10^{-19}$C is the modulus of the electron charge, $\gamma^\mu = (\gamma^0, \gamma^1, \gamma^2)$ are the Dirac matrices, $\partial_\mu = \partial/\partial x^\mu$ is the derivative operator, $x^\mu = (x^0 = v_F t,\ x^1,\ x^2)$ are the space-time coordinates in $1+2$-dimensions, the Fermi velocity $v_F = 10^6$m/s plays the role of the speed of light c and the index μ runs from 0 to 2. The Einstein convention of summing over repeated indices is being used throughout this paper. The Dirac matrices satisfying the anti-commuting relation, $\gamma^\mu\gamma^\nu+\gamma^\nu\gamma^\mu = 2g^{\mu\nu}$, where $g^{\mu\nu} = \mathrm{diag}(1,-1,-1)$ is the Minkowski metric tensor, can be explicitly represented by $\gamma^0 = \tau_z, \gamma^1 = i\tau_y$ and $\gamma^2 = -i\tau_x$, where the Pauli matrices $\vec{\tau} = (\tau_x, \tau_y, \tau_z)$ are related to the sublattice pseudospin. The honeycomb lattice is composed of two triangular sublattices A and B, rotated w.r.t. each other by 180°, such that for the equation $\tau_z\psi = \pm1\psi$, the eigenvalue $+1(-1)$ represents an electron located at the sublattice A (B). As a matter of fact, electrons in graphene have two additional quantum numbers, i.e., the genuine spin, taking on the values $\sigma = (\uparrow, \downarrow)$, and the valley pseudospin $\alpha = \pm1$, related to the two inequivalent points $\mathbf{K}$ and $\mathbf{K}'$ inside the first Brillouin zone of the honeycomb lattice, at which the Dirac equation emerges effectively. In practice, it is possible to neglect scattering mechanisms which would mix the spinors associated with the quantum numbers σ and α; it suffices to study the behavior of a two-component Dirac spinor and multiply the relevant physical quantities, such as conductivity, by a degeneracy factor, which in the present case is 4.

In what follows, the optical analogue of (1) will be obtained through the use of a suitable version of the coupled-mode theory [36]. It is worth to mention that the longitudinal axis of the optical system, denoted by z, plays the role of time t of quantum mechanics [25, 26]. For the sake of completeness, a sketch of the coupled-mode theory will be briefly presented. Starting with the Maxwell equations in the frequency domain for two distinct sets of electromagnetic fields, $(\mathbf{E}, \mathbf{H})$ and $(\mathbf{E}', \mathbf{H}')$, in non-magnetic media ($\mu = \mu_0 = 4\pi\times10^{-7}$H/m) and with dielectric permittivities ε and ε':

$$\nabla\times\mathbf{E} = -i\omega\mu_0\mathbf{H}\,, \tag{2}$$
$$\nabla\times\mathbf{H} = i\omega\varepsilon\mathbf{E}\,, \tag{3}$$
$$\nabla\times\mathbf{E}' = -i\omega\mu_0\mathbf{H}'\,, \tag{4}$$
$$\nabla\times\mathbf{H}' = i\omega\varepsilon'\mathbf{E}'\,, \tag{5}$$

a perturbation expansion can be performed, provided that ε and ε' are only slightly different, i.e., $\varepsilon' = \varepsilon + \delta\varepsilon$, where $\delta\varepsilon$ is a small perturbation to the problem with dielectric permittivity ε, whose solutions are known in exact form. Combining (2)–(5) in a proper way yields the Lorentz reciprocity theorem in non-magnetic media:

$$\nabla\cdot(\mathbf{E}^*\times\mathbf{H}' + \mathbf{E}'\times\mathbf{H}^*) = -i\omega(\varepsilon'-\varepsilon)\mathbf{E}^*\cdot\mathbf{E}'\,. \tag{6}$$

The next step is to perform the volume integration of the above equation and apply the Gauss theorem to a volume defined by a cylinder of radius $r\to\infty$ and height $\Delta z\to0$. The desired result is given below:

$$\int_S \frac{\partial}{\partial z}(\mathbf{E}^*_\perp\times\mathbf{H}'_\perp + \mathbf{E}'_\perp\times\mathbf{H}^*_\perp)\cdot\hat{\mathbf{a}}_z dS = -i\omega\int_S(\varepsilon'-\varepsilon)\mathbf{E}^*\cdot\mathbf{E}' dS\,. \tag{7}$$

where dS is an infinitesimal element of transverse area oriented along the z-direction, $\mathbf{E}_\perp$ and $\mathbf{H}_\perp$ are the transverse components of the electric and magnetic fields, respectively.

Taking $\varepsilon' = \varepsilon$ and inserting two distinct modes, indexed by m and n, given explicitly by:

$$\begin{pmatrix} \mathbf{E} \\ \mathbf{H} \end{pmatrix} = \begin{pmatrix} \vec{\mathcal{E}}_n \\ \vec{\mathcal{H}}_n \end{pmatrix} e^{i(\omega t - \beta_n z)} , \tag{8}$$

$$\begin{pmatrix} \mathbf{E}' \\ \mathbf{H}' \end{pmatrix} = \begin{pmatrix} \vec{\mathcal{E}}_m \\ \vec{\mathcal{H}}_m \end{pmatrix} e^{i(\omega t - \beta_m z)} , \tag{9}$$

where $\vec{\mathcal{E}}_n(x, y)$ and $\vec{\mathcal{H}}_n(x, y)$ carry the full dependence on the transverse coordinates (x, y) and β_n is the propagation constant of the nth mode, one obtains the mode orthogonality relation:

$$\int_S (\vec{\mathcal{E}}^*_{n\perp} \times \vec{\mathcal{H}}_{m\perp} + \vec{\mathcal{E}}_{m\perp} \times \vec{\mathcal{H}}^*_{n\perp}) \cdot \hat{\mathbf{a}}_z dS = \mathrm{sgn}(n)\delta_{mn} . \tag{10}$$

Besides the orthogonality relation, it can be shown that the full set of modes also satisfy a completeness relation, such that any arbitrary electromagnetic field $(\mathbf{E}', \mathbf{H}')$ can be represented as a linear superposition of modes, i.e., the modes form a complete basis in a vector space of functions. Therefore, the solution $(\mathbf{E}', \mathbf{H}')$ for the electromagnetic fields in a dielectric medium described by ε' can be expand in terms of the exactly known modes of a simpler problem with dielectric permittivity ε, as follows:

$$\begin{pmatrix} \mathbf{E}' \\ \mathbf{H}' \end{pmatrix} = \sum_m c_m(z) \begin{pmatrix} \vec{\mathcal{E}}_m \\ \vec{\mathcal{H}}_m \end{pmatrix} e^{i(\omega t - \beta_m z)} , \tag{11}$$

where $c_m(z)$ are the expansion coefficients, which can only depend on the longitudinal coordinate z. Taking into account the orthogonality relation, one gets a system of differential equations for the coefficients $c_n(z)$:

$$i\frac{dc_n}{dz} = \beta_n c_n + \sum_m c_m t_{mn} , \tag{12}$$

where the coupling constants t_{mn} are given by:

$$t_{mn} = \frac{\omega}{2}\mathrm{sgn}(n)\int_S (\varepsilon' - \varepsilon)\vec{\mathcal{E}}_m \cdot \vec{\mathcal{E}}^*_n dS . \tag{13}$$

By inspecting (12), one can clearly observe that it resembles the Schrödinger equation for a tight-binding model, leading to the establishment of a formal analogy with quantum mechanics by postulating the following "Hamiltonian" function:

$$H = \sum_n \beta_n c^*_n c_n + \sum_{mn} t_{mn} c^*_m c_n , \tag{14}$$

where the propagation constant β_n plays the role of energy associated with the nth mode and t_{mn} is the hopping parameter allowing the transition between the mth and nth states.

Now, the optical analogous of the graphene can be obtained by arranging a set of identical circular optical waveguides in a honeycomb lattice, as illustrated in Fig. 1. The core of each waveguide has dielectric permittivity ε_1 and radius r_0, while the external medium has permittivity ε_2. The center-to-center distance between the waveguides is formally known as the lattice constant a. The fundamental mode of a circular waveguide is well approximated by a linearly polarized field having gaussian distribution from the waveguide axis, in the following way:

$$\mathbf{E}_0 = \left(\frac{\omega\mu_0\alpha}{\pi\beta}\right)^{1/2} e^{-\alpha r^2/2} e^{i(\omega t - \beta_0 z)} \hat{\mathbf{e}}_0, \tag{15}$$

where $\hat{\mathbf{e}}_0$ is the polarization unit vector, r is the radial distance from the symmetry axis of the waveguide, β_0 is the fundamental mode propagation constant and, together with the constant α, must be the determined from a rigorous modal analysis. Since the electromagnetic field is confined inside the waveguide core, only first neighbors have appreciable coupling constants t_{mn}, i.e., $t_{mn} = t_0$

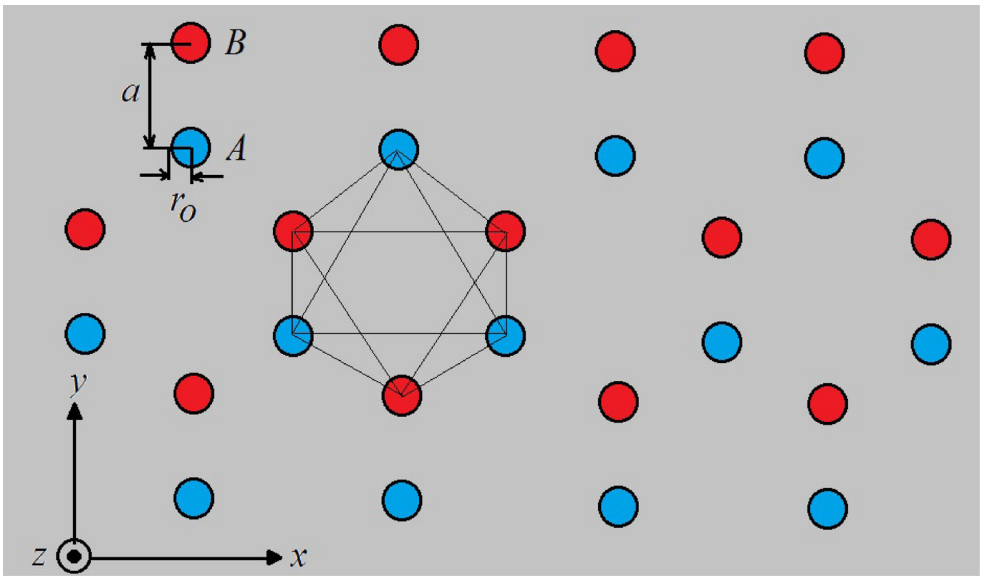

Fig. 1 Sketch of the honeycomb lattice obtained using a set of circular waveguides

for first neighbors, while becoming vanishingly small for higher order neighbors. Therefore, the hopping amplitude t_0 is approximately given by:

$$t_0 = \frac{\omega^2 \mu_0 (\varepsilon_1 - \varepsilon_2)}{\beta_0} e^{-\alpha a^2/2} (1 - e^{-\alpha r_0^2}) \, . \tag{16}$$

Neglecting counter-propagating modes, the Hamiltonian function (14) reduces to:

$$H = \beta_0 \sum_n c_n^* c_n + t_0 \sum_{n,\delta} c_n^* c_{n+\delta} \, , \tag{17}$$

where the first term corresponds to an "energy" constant of the whole system which can be immediately removed by the transformation $c_n(z) = c_n'(z) e^{-i\beta_0 z}$ and the index $\delta = 1, 2, 3$ runs over the first nearest neighbors of the nth waveguide. It is worth mentioning that from the point of view of symmetry and group theory, the honeycomb structure does not form a pure Bravais lattice, i.e., the vectors connecting a given site to its first neighbors cannot be used as basis vectors allowing the reconstruction of the whole lattice by means of pure translations [37]. As a matter of fact, the honeycomb structure is composed of two triangular Bravais sub-lattices A and B, as shown explicitly in Fig. 1. The basis is formed by a waveguide in sub-lattice A and a waveguide in sub-lattice B, with Bravais lattice vectors given by:

$$\mathbf{a}_1 = \sqrt{3} a \hat{\mathbf{x}} \, , \tag{18}$$

$$\mathbf{a}_2 = \sqrt{3} a \left(\frac{1}{2} \hat{\mathbf{x}} + \frac{\sqrt{3}}{2} \hat{\mathbf{y}} \right) \, . \tag{19}$$

Therefore, it is convenient to replace the general coefficients c_n by a_n and b_n, representing the wave amplitude in the nth waveguide of the sub-lattice A and B, respectively, to recast the Hamiltonian (17) into the form below:

$$H = t_0 \sum_{\langle mn \rangle} (a_m^* b_n + b_n^* a_m) \, , \tag{20}$$

where $\langle mn \rangle$ means the sum over first neighbors. The vectors connecting a waveguide in the sub-lattice A to its first neighbors in sub-lattice B are given by:

$$\boldsymbol{\delta}_1 = a \hat{\mathbf{y}} \, , \tag{21}$$

$$\boldsymbol{\delta}_2 = \frac{a}{2} (\sqrt{3} \hat{\mathbf{x}} - \hat{\mathbf{y}}) \, , \tag{22}$$

$$\boldsymbol{\delta}_3 = \frac{a}{2} (-\sqrt{3} \hat{\mathbf{x}} - \hat{\mathbf{y}}) \, . \tag{23}$$

while a waveguide in sub-lattice B is connected to its first neighbors, pertaining to sub-lattice A, by $-\boldsymbol{\delta}_1, -\boldsymbol{\delta}_2, -\boldsymbol{\delta}_3$.

The Hamiltonian (29) can be exactly diagonalized by using the Fourier decomposition of the amplitudes $a_n(z)$ and $b_n(z)$, in the following way:

$$a_n(z) = \frac{1}{\sqrt{N}} \sum_{\mathbf{k}} a_{\mathbf{k}}(z) e^{i \mathbf{k} \cdot \mathbf{r}_n} \, , \tag{24}$$

$$b_n(z) = \frac{1}{\sqrt{N}} \sum_{\mathbf{k}} b_{\mathbf{k}}(z) e^{i \mathbf{k} \cdot \mathbf{r}_n} \, . \tag{25}$$

$$\delta_{\mathbf{k}\mathbf{k}'} = \frac{1}{N} \sum_n e^{i (\mathbf{k} - \mathbf{k}') \cdot \mathbf{r}_n} \, , \tag{26}$$

where N is the total number of waveguides (sites) in each sub-lattice, $\mathbf{k} = (k_x, k_y)$ is a wavevector in two dimensions, $\mathbf{r}_n = (x_n, y_n)$ is the position of the nth waveguide in the (x, y)-plane, $a_{\mathbf{k}}(z)$ and $b_{\mathbf{k}}(z)$ are the Fourier coefficients, and $\delta_{\mathbf{k}\mathbf{k}'}$ is the Kronecker delta function. Insertion of (24) and (25) into (29) and making use of the vectors (21)–(23) yield:

$$H = \sum_{\mathbf{k}} [f_{\mathbf{k}} a_{\mathbf{k}}^* b_{\mathbf{k}} + f_{\mathbf{k}}^* b_{\mathbf{k}}^* a_{\mathbf{k}}] \, , \tag{27}$$

where $f_{\mathbf{k}} = t_0 \sum_n e^{i \mathbf{k} \cdot \boldsymbol{\delta}_n}$. For the sake of convenience, a fictitious spinor in the so-called Nambu representation can be defined as follows:

$$\psi_{\mathbf{k}} = \begin{pmatrix} a_{\mathbf{k}} \\ b_{\mathbf{k}} \end{pmatrix} \, , \tag{28}$$

allowing one to rewrite the Hamiltonian (27) in the following way:

$$H = \sum_{\mathbf{k}} \psi_{\mathbf{k}}^\dagger H_{\mathbf{k}} \psi_{\mathbf{k}} = \sum_{\mathbf{k}} \psi_{\mathbf{k}}^\dagger \begin{pmatrix} 0 & f_{\mathbf{k}} \\ f_{\mathbf{k}}^* & 0 \end{pmatrix} \psi_{\mathbf{k}} \, . \tag{29}$$

The eigenvalues of the matrix $H_{\mathbf{k}}$, corresponding to the energy solutions in the $\mathbf{k}$-space, can be promptly obtained, leading to the emergence to two distinct bands, $E_{\mathbf{k}} = \pm |f_{\mathbf{k}}|$, which touch each other at the so-called Dirac points, obtained from the condition $E_{\mathbf{k}} = 0$. The Dirac points are located at the corners of the first Brillouin zone of a honeycomb lattice, $\mathbf{K} = 4\pi/(3\sqrt{3}a)\hat{\mathbf{x}}$ and $\mathbf{K}' = -4\pi/(3\sqrt{3}a)\hat{\mathbf{x}}$. The function f_k can be linearized at the Dirac point $\mathbf{K} = 4\pi/(3\sqrt{3}a)\hat{\mathbf{x}}$, by expressing $\mathbf{k} = \mathbf{K} - \mathbf{q}$, where $|\mathbf{q}| << |\mathbf{K}|$, which yields:

$$f_{\mathbf{K}-\mathbf{q}} = \frac{3at_0}{2} (q_x - i q_y) \, . \tag{30}$$

For plane wave solutions of the form $\psi(\mathbf{r}, z) \propto e^{i \mathbf{q} \cdot \mathbf{r}}$, from which any general solution can be obtained by linear superposition, it is possible to replace $\mathbf{q}$ by the differential operator $-i \nabla_\perp = -i (\partial_x, \partial_y)$. This way, with the aid of the Pauli matrices τ_x and τ_y the effective Hamiltonian (29) can be written as follows:

$$\hat{H} = v_F \int d^2 \mathbf{r} \psi^\dagger (-i \tau_x \partial_x - i \tau_y \partial_y) \psi \, , \tag{31}$$

where $\psi(\mathbf{r}, z)$ is a two-component Dirac spinor and $v_F = 3at_0/2$ plays the role of a "Fermi velocity" (notice, however, that it is actually dimensionless). Finally, by means of the Legendre transform, the above Hamiltonian is related to the following lagrangian density:

$$\mathcal{L} = iv_F\bar{\psi}\gamma^\mu\partial_\mu\psi \ , \tag{32}$$

where $\bar{\psi} = \psi^\dagger\gamma^0$ is the adjoint spinor, $\gamma^\mu = (\tau_z, i\tau_y, -i\tau_x)$ are the Dirac gamma matrices, and $\partial_\mu = (v_F^{-1}\partial_z, \partial_x, \partial_y)$. It is worth pointing out again that, in the present context, the coordinate z plays the role of time t. A gauge potential A_μ in optics is related to the variation of the refractive index, as discussed in ref. [25], leading to an equation of motion analogous to (1), provided that the time t is replaced by the longitudinal coordinate z. The spatial variation of the refractive index in isotropic and linear medium can be entirely accounted by the scalar potential A_0 alone, setting $A_x = A_y = 0$. For the sake of simplicity, only that case will be considered here, leading to the following equation:

$$iv_F\gamma^\mu\partial_\mu\psi + \gamma^0 A_0\psi = 0. \tag{33}$$

To finish the present section, we must emphasize that the set of waveguides must be properly operated by exciting the optical system around the point $\mathbf{K}$ (or equivalently $-\mathbf{K}$, i.e., the corners of the Brillouin zone of the photonic crystal). This means that incident light at $z = 0$ must have an initial angle θ_0 w.r.t. the z-axis, such that $\tan\theta_0 = |\mathbf{K}|/\beta_0$, since the wavefunctions have the complete form $\psi \propto e^{-i\beta_0 z + i\mathbf{K}\cdot\mathbf{r}}$. Small variations $\delta\theta$ around the value θ_0, excite the modes with wavevectors $\mathbf{K} - \mathbf{q}$, whose description is effectively given by the above equation. Using typical values in the near IR spectrum, the vacuum wavelength is of order $\lambda_0 = 1\mu$m and the effective refractive index of the glass for the fundamental mode is around $n = 1.4$, for which we obtain $\beta_0 = k_0 n \approx 2\pi n/\lambda_0 \approx 2.4\times10^6$ rad/m. The lattice constant a can be taken as 100μm implying that $\theta_0 \sim 0.15°$. Current lightwave technology certainly can deal with such precise angle values. Typical acceptance angle θ_{max} from air to the optical waveguides is approximately given by $\sqrt{2\Delta} \approx 1°$, where $\Delta = (n_1 - n_2)/n_1 \sim 10^{-4}$ is the refractive index difference from core to the nearby environment. The angle of incidence θ_0 must lie within the range $0 \le \theta_0 \le \theta_{max}$. This way, the last condition can be satisfied in our model.

3 Conclusion

In summary, in the present contribution, using the coupled mode theory, we demonstrated the possibility of emulating graphene physics using current lightwave technology. The optical system is based on a photonic crystal consisting of a set of circular waveguides arranged in the form of a honeycomb lattice. It important to emphasize that the longitudinal axis z plays the role of time t in our approach. This way an equation formally analogous to the Dirac equation for massless fermions in $(1+2)$D emerges quite naturally. As a final remark, we must point out that there exists a fundamental distinction between the Dirac equation in graphene and its optical analogue, which is the fact the electrons are actually fermions. The fermionic nature of electrons clearly shows up when the Dirac field is quantized, but such feature cannot be captured by light, at least in the present formulation.

Acknowledgments The authors would like to thank the brazilian agency CNPq for partial financial support.

References

1. K.S. Novoselov, A.K. Geim, S.V. Morozov, D. Jiang, Y. Zhang, S.V. Dubonos, I.V. Grigorieva, A.A. Firsov, Science **306**, 666 (2004)
2. P.R. Wallace, Phys. Rev. **71**, 622 (1947)
3. J.W. McLure, Phys. Rev. **108**, 612 (1957)
4. G.W. Semenoff, Phys. Rev. Lett. **53**, 2449 (1984)
5. K.S. Novoselov et al., PNAS **102**, 10451 (2005)
6. K.S. Novoselov et al., Science **306**, 666 (2004)
7. A.H. Castro Neto et al., Rev. Mod. Phys. **81**, 109 (2009)
8. S. Das Sarma et al., Rev. Mod. Phys. **83**, 407 (2011)
9. M.A.H. Vozmediano, M.I. Kastnelson, F. Guinea. Physics Reports **496**, 109 (2010)
10. C.A. Dartora, G.G. Cabrera. Phys. Lett. A **377**, 907 (2013)
11. C.A. Dartora, G.G. Cabrera, Phys. Rev. B **87**, 165416 (2013)
12. K.S. Novoselov et al., Nature **438**, 197 (2005)
13. Y. Zhang, Y.-W. Tan, H.L. Stormer, P. Kim, Nature **438**, 201 (2005)
14. M.R. Setare, D. Jahani, Physica B **405**, 1433 (2010)
15. N. Bolivar, E. Medina, B. Berche, Phys. Rev. B **89**, 125413 (2014)
16. A. Lopez Jimenez, N. Bolvar, E. Medina, B. Berche, Condens. Matter Phys. **17**, 33803 (2014)
17. M.I. Kastnelson, K.S. Novoselov, A.K. Geim, Nat. Phys. **2**, 620 (2006)
18. M.I. Kastnelson, K.S. Novoselov, Solid State Commun. **143**, 3–13 (2007)
19. J.D. Lejarreta, C.H. Fuentevilla, E. Diez, J.osé.M. Cerveró, *J. Phys. A: Math. Theor. 46* (155304, 2013)
20. E. Yablonovitch, Phys. Rev. Lett. **58**, 2059–2062 (1987)
21. S. John, Phys. Rev. Lett. **58**, 2486–2489 (1987)
22. K. Ohtaka, Phys. Rev. B **19**, 5057–5067 (1979)
23. E. Yablonovitch, T.J. Gmitter, K.M. Leung, E. Gmitter, T.J. Leung, Phys. Rev. Lett. **67**, 2295–2298 (1991)
24. T.F. Krauss, R.M. DeLaRue, S. Brand, Nature **383**, 699–702 (1996)
25. C.A. Dartora, G.G. Cabrera, K.Z. Nobrega, V.F. Montagner, M.H.K. Matielli, F.K. Rodrigues de Campos, H.T.S. Filho, Phys. Rev. A **83**, 012110 (2011)
26. C.A. Dartora, K.Z. Nobrega, G.G. Cabrera, Phys. Lett. A **375**, 2254–2257 (2011)
27. M. Mehrafarin, H. Balajany, Phys. Lett. A **374**, 1608–1610 (2010)
28. A.V. Nalitov, G. Malpuech, H. Tercas, D.D. Solnyshkov, Phys. Rev. Lett. **114**, 026803 (2015)

29. J. Böhm, M. Bellec, F. Mortessagne, U. Kuhl, S. Barkhofen, S. Gehler, H.-J. Stöckmann, I. Foulger, S. Gnutzmann, G. Tanner, Phys. Rev. Lett. **114**, 110501 (2015)
30. M. Bellec, U. Kuhl, G. Montambaux, F. Mortessagne, Phys. Rev. B **88**, 115437 (2013)
31. M. Bellec, U. Kuhl, G. Montambaux, F. Mortessagne, Phys. Rev. Lett. **110**, 033902 (2013)
32. G. Weick, C. Woollacott, W.L. Barnes, O. Hess, E. Mariani, Phys. Rev. Lett. **110**, 106801 (2013)
33. D. Dragoman, J. Opt. Soc. Am. B **27**, 1325 (2010)
34. L.H. Ryder, *Quantum Field Theory, 2nd. ed* (University Press, Cambridge, 1996)
35. S. Weinberg, *The Quantum Teory of Fields, Vol. I and II* (University Press, Cambridge, 1996). and references therein
36. H.A. Haus, W.P. Huang, S. Kawakami, N.A. Whitaker, J. Lightwave Technol. **5**, 16–23 (1987)
37. M. Tinkham, *Group Theory and Quantum Mechanics* (Dover Publications, New York, 2003)